Kinetics and Product Study of the Reaction of CH_3 Radicals with $O(^3P)$ Atoms Using Time Resolved Time-of-Flight Spectrometry

Christopher Fockenberg,* Gregory E. Hall, Jack M. Preses, Trevor J. Sears, and James T. Muckerman

Chemistry Department 555A, Brookhaven National Laboratory, P.O. Box 5000, Upton, New York 11973-5000

Received: April 6, 1999; In Final Form: May 17, 1999

The kinetics and product distribution for the reaction of methyl radicals, CH_3, with ground-state $O(^3P)$ oxygen atoms have been investigated. This reaction was studied with a newly constructed apparatus combining a tubular flow reactor and a time-of-flight mass spectrometer (TOFMS), using a hollow-cathode lamp for photoionization. The radicals are produced by an excimer laser pulse ($\lambda = 193$ nm) in the cophotolysis of acetone, CH_3COCH_3, or bromomethane, CH_3Br, and sulfur dioxide, SO_2, creating a homogeneous distribution of radicals along the axis of the flow reactor. A small fraction of the reaction mixture is sampled through a pinhole in the wall. Subsequent ionization and repeated extraction of ionized molecules into the TOFMS at a high repetition rate ($\approx$20 kHz) allows the simultaneous observation of rapid changes in the concentration of multiple species in the flow reactor. In addition to the dominant product, formaldehyde (CH_2O), carbon monoxide (CO) was detected as a product with a yield of 0.17 ± 0.11. Analysis of the rate of disappearance of methyl radicals and appearance of formaldehyde for different $O(^3P)$ concentrations resulted in an overall rate coefficient for this reaction $k = (1.7 \pm 0.3) \times 10^{-10}$ cm^3 molecule^{-1} s^{-1} at $T = (299 \pm 2)$ K and $P =$ 1 Torr (He).

Introduction

The combustion of methane is of considerable importance in the generation of energy. The oxidation of methane starts with a chain initiation process in which a hydrogen atom is abstracted. Under lean-to-moderately rich conditions the methyl radicals produced react predominantly with oxygen atoms:[1,2]

$$CH_3 + O(^3P) \rightarrow \text{products} \qquad (1)$$

The kinetics of this reaction have been studied extensively[3−7] by observing either the disappearance of methyl radicals in the presence of oxygen atoms or the formation of formaldehyde as the major product. The overall rate coefficient for reaction 1 has been observed to be $(1.4 \pm 0.3) \times 10^{-10}$ cm^3 molecule^{-1} s^{-1}, independent of pressure and temperature.[8] However, only a few investigations with regard to the product distribution were performed. There are several exothermic channels and one endothermic product channel for this reaction:[9,10]

$$CH_3 + O \rightarrow CH_2O + H \qquad \Delta H = -294.1 \text{ kJ/mol} \qquad (1a)$$

$$\rightarrow HCO + H_2 \qquad \Delta H = -354.2 \text{ kJ/mol} \qquad (1b)$$

$$\rightarrow CO + H + H_2 \qquad \Delta H = -228.7 \text{ kJ/mol} \qquad (1c)$$

$$\rightarrow CH + H_2O \qquad \Delta H = -43.9 \text{ kJ/mol} \qquad (1d)$$

$$\rightarrow OH + CH_2 \qquad \Delta H = +29.2 \text{ kJ/mol} \qquad (1e)$$

Niki et al.[3] performed flow tube measurements in which methyl radicals were produced in the reaction of ethylene with oxygen atoms:

$$C_2H_4 + O \rightarrow CH_3 + HCO \qquad (2)$$

The reactants were detected by mass spectrometry. The reported yield of formaldehyde from reaction 1 was larger than 0.85. Water as a possible byproduct was not detected, thus ruling out channel (1d). However, reaction 2 does not seem to be a clean source for methyl radicals.[11] According to Koda et al.[12] another, equally important product of this reaction is CH_2CHO, which could also lead to CH_2O in the reaction with oxygen atoms, thus altering the measured yield of formaldehyde. Slagle et al.[6] used a different approach for generating methyl radicals and oxygen atoms. The radicals were produced by the photolysis of acetone and SO_2, respectively. A photoionization mass spectrometer was used as an analytical tool. Although a Ne resonance lamp served as a source of VUV radiation ($h\nu =$ 16.67 and 16.85 eV) for ionization, no attempt to detect CO (ionization energy (IE) = 14.01 eV)[13] was reported. However, neither HCO nor CH_2 radicals were found, rendering channels 1b and 1e negligible. It was concluded that 1a was the only open channel at temperatures between 294 and 900 K.

Fairly recently, Seakins and Leone[14] performed a product study focusing on CO as a possible reaction product. They applied essentially the same method for generation of the reactants as did Slagle et al., but instead used a time-resolved FTIR emission technique to detect reaction products. From these infrared emission studies they could clearly identify vibrationally excited CO as a product of reaction 1 with a nascent population of up to $v = 8$. They determined an overall yield for CO from reaction 1 of 0.4 ± 0.2. This would definitely indicate that channel 1c cannot be neglected as a direct route for producing CO.

We have chosen to investigate reaction 1 to test the capabilities of our new apparatus and to attempt to resolve the discrepancy concerning the branching ratios for reaction 1. We

* Author to whom correspondence should be addressed.

10.1021/jp991157k CCC: $18.00
Published on Web 06/24/1999

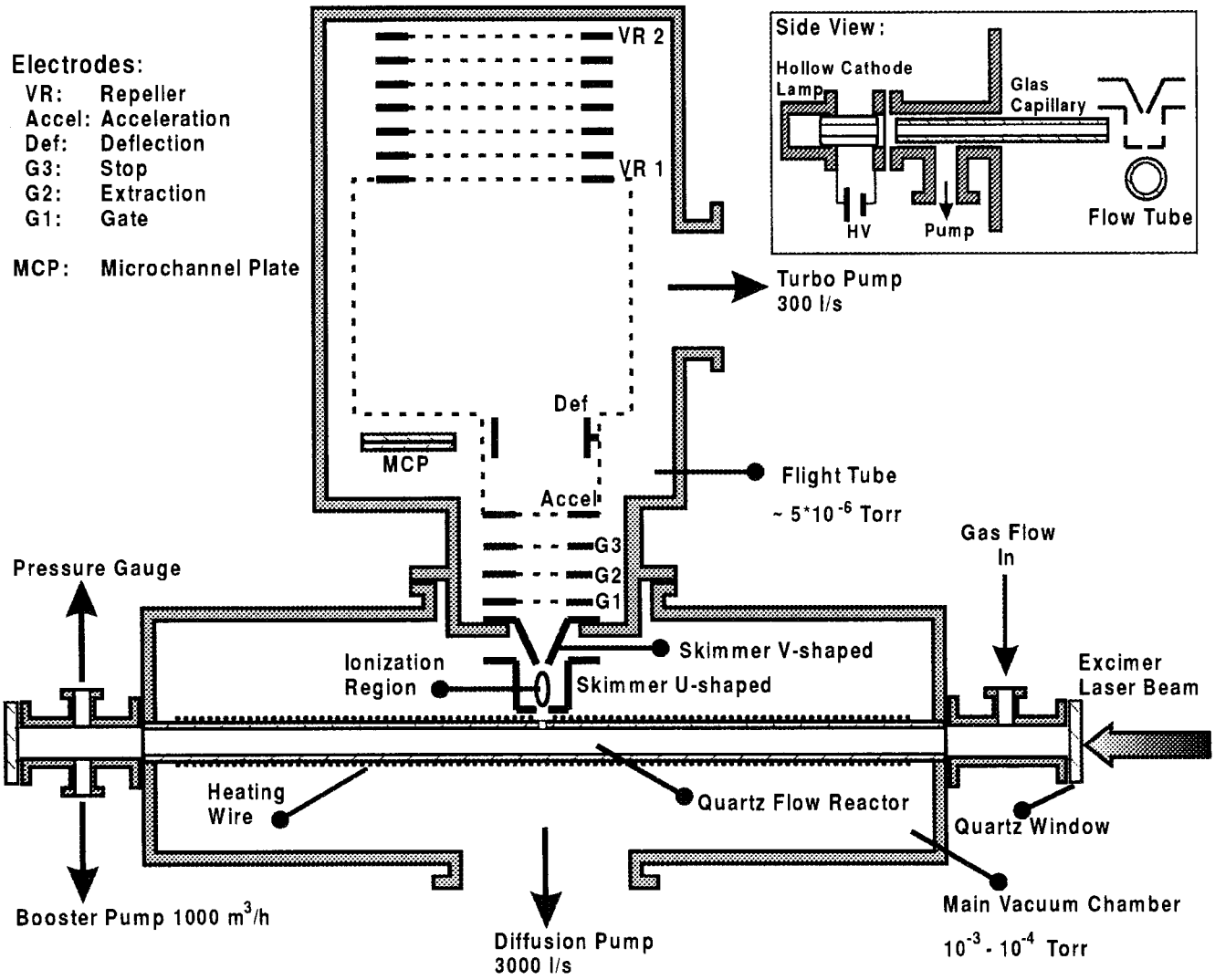

Figure 1. Schematic diagram of the apparatus.

will present results for the rate coefficient that agree well with previously measured values and show evidence for the existence of channel 1c, supporting the findings of Seakins and Leone. These measurements will demonstrate the suitability of this new technique for this type of experiment.

We want to focus our research on radical−radical reactions, which are especially challenging to investigate because potential side and chain reactions may complicate the data analysis greatly. Moreover, the recombination of two radicals frequently produces highly excited adducts that open up more than one product channel. To fully characterize a reaction, one needs to observe more than a single species involved in the reaction. Ideally, all participant species should be detected simultaneously, eliminating assumptions about the concentrations of unobserved molecules that are made in experiments with single-species detection.

Our experimental setup resembles the one that Slagle et al.[6,15−17] designed with one important exception—instead of using a quadrupole mass spectrometer we analyze sampled gas from the photolysis reactor by time-of-flight mass spectrometry (TOFMS). Thus, direct information on product distributions as well as reaction rates can be obtained in a single experiment.

Experimental Section

A detailed description of the apparatus will be published elsewhere[18] and only an overview will be given here. Radicals are produced in a tubular quartz reactor by photolysis of suitable precursor molecules. Precursors, reactants, and products are sampled continuously by allowing gas to escape from the reactor through a pinhole in the wall, into a region where a portion of the sampled gas is photoionized. By switching voltages on a grid assembly at the entrance to the time-of-flight mass spectrometer [TOFMS: R. M. Jordan Co., D850 Reflectron with a microchannel plate detector (MCP): C-726] ions can enter the TOF chamber during a brief time interval (≈12 μs). The gating/extraction procedure can be carried out at a high rate (∼20 kHz) enabling us to take "snapshots" of the composition of the reaction mixture in intervals of 48 μs. This interval was chosen from the possible choices afforded by the hardware so that species up to a mass of 150 amu can be acquired without interference from neighboring mass spectra. Rapid changes in concentration due to reactions can therefore be observed on a millisecond time scale. Figure 1 shows a schematic diagram of the apparatus.

Apparatus. The reaction vessel consists of a 43 cm long quartz tube with an inner diameter of approximately 1 cm. The sample orifice (1 mm in diameter) is located roughly in the middle of the tube. The whole reactor is placed inside a vacuum chamber pumped by an oil diffusion pump backed by a rotary pump. Connections for a gas inlet and outlet were attached to flanges on either side of the vacuum chamber also bearing quartz windows through which radiation from an excimer laser

(Lambda Physik, LPX 240iMC) was directed into and out of the reactor. The rectangular cross section of the emitted laser radiation was reduced to a square shape by a Galilean telescope made of cylindrical quartz lenses. Typical energies were ~100 mJ/pulse at the laser, with 30 mJ/pulse exiting the reactor without any absorber present in the flow tube. The main loss of beam intensity was caused by the windows and lenses. The remaining losses could be attributed to absorption by ambient oxygen in the pathway and the divergence of the laser beam leaving the flow tube. However, the divergence was sufficiently low to produce a uniform distribution of radicals along the tubular reactor from its entrance to the sampling orifice. Intensity measurements made at the exit window of the flow tube automatically take atmospheric O_2 absorption into account.

A gas mixture composed of precursor molecules for the radicals as well as bath gas was passed through the tube where a constant flow was established by a set of three mass-flow controllers (Tylan General, FC 260). The pressure in the flow reactor was controlled by throttling the gas flow through a gate valve at the downstream end of the reactor. Typical flow velocities ranged from 10 to 20 m/s.

Gas that left the tube through the orifice first passed through a U-shaped skimmer that had windows cut into its wall through which the ionizing radiation emitted from a hollow-cathode lamp (McPherson, Model 630) was directed. The lamp was operated with either Ne ($h\nu$ =16.67 and 16.85 eV) or Ar ($h\nu$ = 11.62 and 11.83 eV) in the discharge at low pressures ($p \leq 400$ mTorr). A glass capillary, which also acts as a differential pumping barrier, is used to guide the photons from the lamp to the ionization region. The TOF chamber is pumped by a turbomolecular pump. Starting a few hundred microseconds before each laser shot, a sequence of 85−170 mass spectra were typically acquired covering 4−8 ms. After averaging typically 100 000 to 200 000 laser shots, the counts under each mass peak were then integrated and the sum was plotted against the time relative to the laser initiation.

To check for fluctuations in the detection efficiency of the apparatus, calibration measurements on absolute concentrations of the main stable species involved in this study were done on a daily basis. Although the determined calibration coefficients could vary by more than 20% from day to day, the cracking pattern of any species in the photoionization process were very reproducible.

Experiment. For the investigation of the reaction of methyl radicals with oxygen atoms we used either acetone or bromomethane as precursor species for methyl radicals, whereas oxygen atoms were generated by the photolysis of SO_2:

$$CH_3COCH_3 + h\nu\ (193\ \text{nm}) \rightarrow 2CH_3 + CO \qquad (3)$$

$$CH_3Br + h\nu\ (193\ \text{nm}) \rightarrow CH_3 + Br \qquad (4)$$

$$SO_2 + h\nu\ (193\ \text{nm}) \rightarrow SO + O(^3P) \qquad (5)$$

All gases were stored as dilute mixtures in He in 20 L glass bulbs, except SO_2, which was purchased as a 5% mixture in He (Praxair, purity: $SO_2 \geq 99.6\%$, He UHP-grade). Prior to use, acetone (Mallinckrodt, purity 99.7%) was degassed in several freeze−pump−thaw cycles, released into the storage vessel, and pressurized with He (Praxair, UHP grade). The concentration ratio was determined according to the partial pressures (MKS Baratron Model 622). Bromomethane (Matheson, purity > 99%) was used without purification.

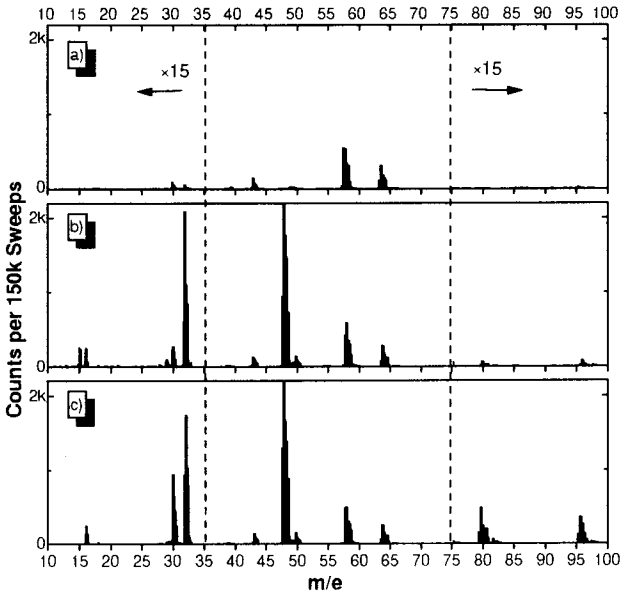

Figure 2. Averaged TOF spectra recorded in experiment #22 (see Table 2) using Ar emission for ionization. 150000 sweeps were co-added for a single mass spectrum. (a) The mass spectrum of the mixture before the laser pulse; (b) the mass spectrum taken 240 μs after the photolysis pulse; (c) the mass spectrum after all methyl radicals were consumed. The signal below m/e = 35 and above m/e = 75 is multiplied by a factor of 15 for clarity.

For reference measurements, mixtures of CO (Matheson, purity > 99%) and CH_2O with He were prepared in 3 L glass bulbs. Formaldehyde was made by heating para-formaldehyde (Aldrich) to a temperature around 100 °C. CH_2O was collected in a liquid nitrogen trap, transferred to a glass bulb on warming, and diluted with He. Typically, this was performed a sufficiently long time before use to ensure complete mixing (at least 5 h), but not so long as to lose formaldehyde through polymerization.

Typical concentrations in the reactor were $(0.5-1.0) \times 10^{14}$ molecules cm^{-3} (1.5−3.0 mTorr) for SO_2 or CH_3Br, and $(0.5-1.5) \times 10^{13}$ molecules cm^{-3} (0.15−0.45 mTorr) for acetone. At laser pulse energies of 15−30 mJ/cm^2 (λ = 193 nm), measured behind the exit window of the reactor tube, 10−20% of the SO_2, approximately 1.5% of the CH_3Br, and 3−6% of the acetone were photolyzed typically. The attenuation of the laser beam due to absorption in the reactor was small and therefore was not suitable for a quantitative determination of radical concentrations formed in the photolysis. Instead, the initial concentrations of radicals were calculated according to the relative drop in signal multiplied by the concentration of precursor molecules (see Figure 4). Unfortunately, the small loss of bromomethane was almost completely buried in the scatter of the CH_3Br signal so that only estimates of the methyl radical concentration could be given when this source of methyl radicals was used. On the basis of the absorption coefficients for CH_3Br and SO_2[8,19,20] and the actual concentration of both species in the reactor, one can also calculate the relative drop in the CH_3Br concentration assuming a quantum efficiency of unity for dissociation for both molecules. The measured and the calculated values agree very well. The overall pressure in the reactor was generally 1 Torr He at a flow velocity of 10−20 m/s. The laser was pulsed at a rate of 8−10 Hz. During an experiment, the energy per pulse of the excimer laser, flow controller values, temperature, pressure, and the intensity of the ionization radiation were constantly recorded. The TOF data were normalized for differences in excimer pulse energy and hollow cathode lamp emission where necessary.

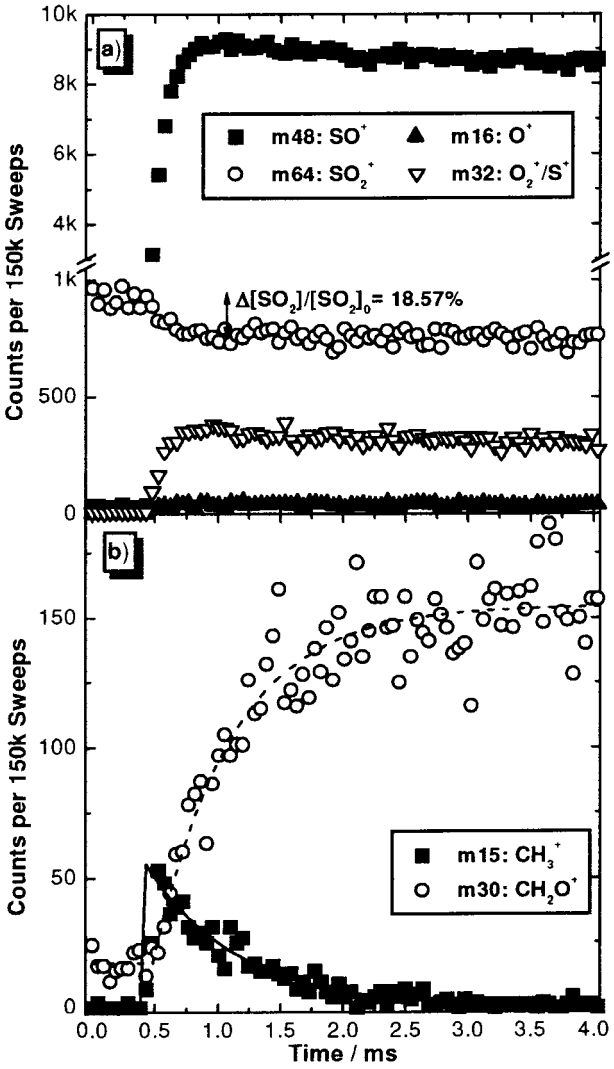

Figure 3. Ion signals plotted vs time for several species acquired in experiment #22 (see Figure 4 and Table 2). The lines in plot (b) are fits of simple exponential decay and rise functions to the data. The calculated first-order rate constants are $k' = 1390\ s^{-1}$ (—) and $k'' = 1590\ s^{-1}$ (- - -).

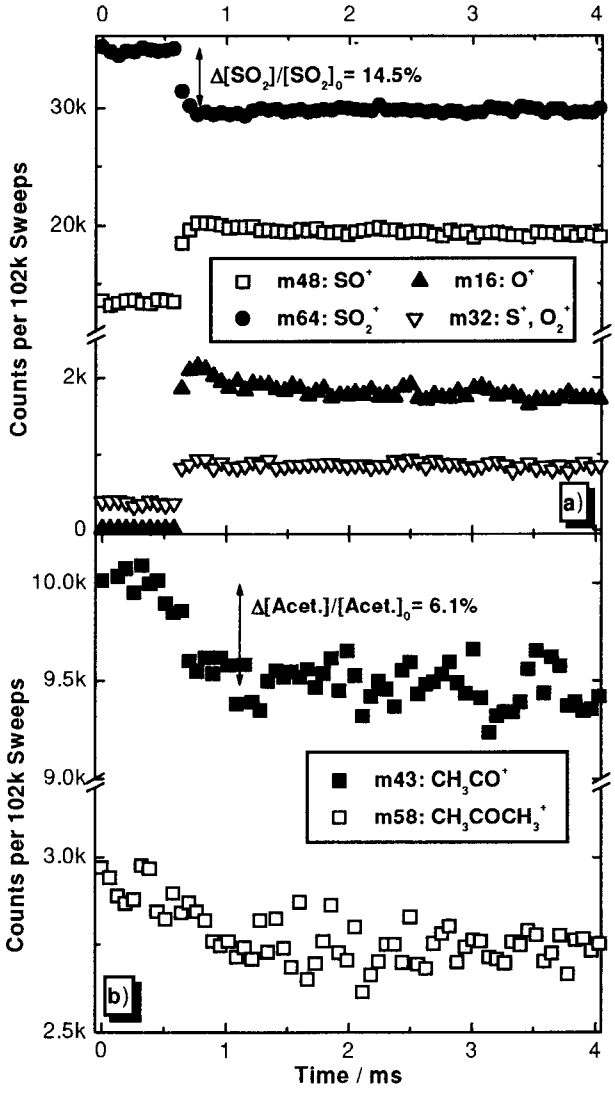

Figure 4. Ion signals associated with $O(^3P)$, SO_2, and acetone plotted vs time acquired in experiment # 5 (see Table 2) using Ne emission for ionization.

Two noble gases were used as discharge media for the hollow cathode lamp, delivering mainly photons of either 16.67/16.85 eV (Ne) or 11.62/11.83 eV (Ar). Even though SO_2 (IE = 12.5 eV)[21] should not be ionized using Ar, a signal could be clearly detected at $m/e = 64$ (see Figure 2). This might be explained by a contamination of the primary emission with shorter wavelength radiation, emitted perhaps from ionized Ar. This might also cause the occurrence of a signal at $m/e = 32$ after SO_2 was photolyzed producing SO (IE = 10.29 eV)[22] and $O(^3P)$ (IE = 13.62 eV)[23] (see Figure 3). Highly excited SO^+ ions might crack into S^+ ions [IE(S) = 10.36 eV][23] and oxygen atoms, although there should not be enough energy available for ionization and dissociation after absorption of one photon. The general advantage of using longer-wavelength radiation for ionization is that cracking is reduced or eliminated. The dissociation of ionized acetone [IE = 9.7 eV,[24] appearance potential (AP) for CH_3^+ $AP(CH_3^+) = 15.6$ eV,[25] $AP(CH_3CO^+) = 10.5$ eV[24]] into CH_3^+ ions did not occur, leaving the $m/e = 15$ channels (IE = 9.84 eV)[26] essentially free from background. Similarly, low background signals could be collected for CH_2O ($m/e = 30$, IE = 10.88 eV)[27] (see Figure 2). However, CO (IE = 14.01 eV)[13] could not be detected at this photon energy, so that only reaction rates and not branching ratios could be analyzed in these experiments.

Calibration of Concentration. When Ne was used as the discharge gas, the photon energy exceeded the threshold for ionization and dissociation of almost all parent molecules. To determine the quantitative amount of each cracking channel, mass spectra of each individual species were recorded in separate experiments. These measurements were usually carried out by acquiring mass spectra of the selected species at different concentrations. The counts under each mass peak were summed up and plotted against the concentration. A linear fit through these points gives the individual absolute calibration coefficients, CC(a,n), for a specific cracking channel "n" of molecule "a". However, the absolute values of the calibration coefficients depend on a number of different parameters (temperature, pressure, photoionization wavelength and intensity, etc.) which could differ quite substantially over an extended period of time. To eliminate these variations it is easier to work with ratios of calibration coefficients, CR(a,m:b,n) = CC(a,m)/CC(b,n), which are only dependent on the wavelength of the ionizing radiation. Since one of our main interests lies in determining relative product yields, which depend only on concentration ratios, this restriction has no influence on the analysis. Concentration ratios

TABLE 1: Calibration Ratios for CO, CH_2O, and Acetone at an Ionization Photon Energy = 16.67/16.85 EV (Ne)[a]

molecule channel	acetone 15	acetone 28	acetone 29	CO 28	CH_2O 28	CH_2O 29	CH_2O 30
CH_2O 30				1.368 ± 0.14	0.172 ± 0.014	1.237 ± 0.08	1
acetone 43	0.09 ± 0.01	0.00958 ± 0.00134	0.017 ± 0.0015	0.255 ± 0.01			0.206 ± 0.04

[a] Ratios were calculated by dividing the individual calibration constants of molecules in top row through those in the first column.

can be determined via:

$$\frac{[a]}{[b]} = \frac{C(a,m)}{CC(a,m)} \Big/ \frac{C(b,n)}{CC(b,n)} = \frac{C(a,m)}{C(b,n)} \Big/ CR(a,m:b,n)$$

where $C(i,j)$ denotes measured counts in channel m/e = "j" of molecule "i". Some of these ratios are listed in Table 1 for different acetone, CO, and CH_2O channels compared to the m/e = 43 channel of acetone and the m/e = 30 channel of formaldehyde. These calibration experiments were routinely performed with different mixtures.

Kinetic Analysis. The concentrations of the precursor species (CH_3COCH_3/CH_3Br and SO_2) were chosen so that the oxygen atom concentration was always in excess of the methyl radical concentration resulting in $[O]/[CH_3]$ ratios ranging from 7 to 50. For the "highest" concentrations of methyl radicals ($[O]/[CH_3] \leq 10$) the data were treated according to second-order kinetics, whereas pseudo-first-order conditions were assumed for lower methyl concentrations. However, the difference in rate coefficients calculated with both methods was always smaller than 10%, which lay well inside the range of experimental scatter. Also, heterogeneous loss of oxygen atoms, methyl radicals, or any other species on the reactor wall could be neglected on the time scale of the reaction ($\tau \leq 4$ ms). In cases where Ne was used in the hollow cathode lamp, the concentration of oxygen atoms could be observed directly. Practically no loss of oxygen atoms could be detected in any experiment; this was also assumed to be valid when Ar emission was used for photoionization and oxygen atoms could not be ionized.

Interestingly, mass peaks at m/e = 80 and 96 (see Figure 2) suggest the existence of slow side reactions involving sulfur-containing compounds. The signal at m/e = 96 can be explained by the slow recombination of two SO molecules ($k_6 = 4.4 \times 10^{-31}$ cm^6 molecule^{-2} s^{-1})[28] generating S_2O_2 in small concentration compared to SO:

$$SO + SO + M \rightarrow S_2O_2 + M \quad (6)$$

The channel at m/e = 80 can have its origin either in SO_3^+ (IE = 13.15 eV)[21] or S_2O^+ (IE = 10.6 eV)[22] ions. However, the recombination of oxygen atoms with sulfur dioxide is too slow to produce detectable amounts of SO_3 within the observation time ($k_7 = 1.0 \times 10^{-33}$ cm^6 molecule^{-2} s^{-1}):[29]

$$O + SO_2 + M \rightarrow SO_3 + M \quad (7)$$

Slagle et al.[6] detected very small amounts of sulfur atoms produced in the photolysis of SO_2 which might undergo reactions with SO or SO_2 to form S_2O. Unfortunately, the literature on reactions involving S atoms is very sparse, and this particular channel remains unconfirmed.

The slight decay in the concentration of methyl radicals in experiments without SO_2 can be explained easily by the radical recombination reaction:

$$CH_3 + CH_3 + M \rightarrow C_2H_6 + M \quad (8)$$

However, the rate coefficient of this reaction has an upper value of only $\leq 5 \times 10^{-11}$ cm^3 molecule^{-1} s^{-1} at pressures at and below 1 Torr.[11] In addition, the CH_3 concentration is so small compared to the oxygen concentration that the rate of recombination of methyl radicals is negligible with regard to the rate of their reaction with $O(^3P)$. The maximum acceleration of the measured reaction rate due to reaction 8 can be estimated to be only 5% for $[O]/[CH_3] \approx 7$.

Other reactions (reactions 9−12), that might interfere directly or indirectly are too slow under the experimental conditions to have a measurable influence on the acquired profiles.[11,30,31]

$$CH_3 + SO\ (+ M) \rightarrow \text{products}\ (+ M) \quad (9)$$

$$CH_3 + SO_2\ (+ M) \rightarrow \text{products}\ (+ M) \quad (10)$$

$$H + CH_3Br \rightarrow CH_3 + HBr \quad (11)$$

$$O + CH_2O \rightarrow OH + HCO \quad (12)$$

SO and SO_2 might react with methyl radicals, but no decrease in either signal was observed in any experiment. In addition, the possible recombination channels of reactions 9 and 10 should show up at m/e = 63 and 79, respectively, which were not detected. These observations are supported by findings of Slagle et al.[6] who investigated the title reaction under similar conditions and concluded that reactions 9 and 10 can be neglected.

Therefore, in the case of pseudo-first-order conditions, both the decay of the methyl radicals and the rise of formaldehyde as the major product of reaction 1 could be generally fitted to simple exponential functions according to

$$C(CH_3) = [CH_3]_0 \times e^{-k't}$$

$$C(CH_3) = [CH_2O]_{max} \times (1 - e^{-k''t})$$

Under second-order conditions the following two expressions were used to model the CH_3 and CH_2O signal profiles:

$$C(CH_3) = [CH_3]_0 \times \frac{[O]_0 - [CH_3]_0}{[O]_0} \times \frac{e^{-\bar{k}'t}}{1 - \frac{[CH_3]_0}{[O]_0} e^{-\bar{k}'t}}$$

$$C(CH_2O) = [CH_2O]_{max} \times \left(1 - \frac{[O]_0 - [CH_3]_0}{[O]_0} \times \frac{e^{-\bar{k}''t}}{1 - \frac{[CH_3]_0}{[O]_0} e^{-\bar{k}''t}} \right)$$

where $\bar{k} = k \times [O]_0 \times (1 - [CH_3]_0/[O]_0)$. $[CH_3]_0/[O]_0$ ratios were obtained from the initial radical concentrations (see Table 2). In the data analysis, $[CH_3]_0$ and k' were floated freely, whereas $[CH_2O]_{max}$ was determined by averaging the last data points in the time profile and only k'' was fitted (see Figures 3b and 5a,b). The first-order rate constants, k' and k'', were then plotted against the oxygen atom concentration and fitted to a straight line whose slope gave the second-order rate coefficient (see Figure 6). For the Ar-lamp experiments, signals at m/e = 15 and 30 were identified to be CH_3^+ (IE = 9.84 eV,[26] AP-(CH_2^+) = 15.09 eV[32]) and CH_2O^+ (IE = 10.88 eV,[27] AP-

TABLE 2: Experimental Conditions, Calculated Product Yields, and First-Order Rate Constants[a]

#	P_{total}, Torr	T, K	VUV gas	$[SO_2]$, 10^{13}cm^{-3}	[precursor], 10^{13}cm^{-3}	$[CH_3]$, 10^{11}cm^{-3}	$[O(^3P)]$, 10^{12}cm^{-3}	CO yield, %	CH_2O yield, %	k' (CH_3), s^{-1}	k'' (CH_2O), s^{-1}
1	1	300	Ne	10.4	10.4[a]	≈1.5	20.4	18.1 ± 4.0			2909
2	1	300	Ne	15.0	9.0[a]	≈1.3	27.2	17.9 ± 5.1			3887
3	1	395	Ne	8.53	6.27[a]	≈0.9	14.0	16.1 ± 7.0			2637
4	1	300	Ne	7.26	1.13[b]	14.4	12.3	14.2 ± 7.8	76.6 ± 23	1901	2193
5	1	300	Ne	10.1	1.61[b]	19.7	14.6	14.9 ± 9.6	77.0 ± 23	2521	3220
6	1	300	Ne	6.14	0.725[b]	7.97	8.7	12.5 ± 10.1	72.3 ± 22	1099	1678
7	1	299	Ne	6.7	6.46[a]	≈1.0	11.2	18.0 ± 5.4			2652
8	1	299	Ne	8.48	8.07[a]	≈1.4	14.1	20.2 ± 5.0			4547
9	1	299	Ne	10.1	10.1[a]	≈1.7	17.2	17.5 ± 4.5			4426
10	1	298	Ne	5.35	5.05[a]	≈0.9	8.84	13.6 ± 14			2194
11	1	299	Ne	6.07	0.65[b]	6.3	11.7	29.7 ± 4.8	86.8 ± 26	2029	2723
12	1	299	Ne	8.28	0.91[b]	7.9	15.1	29.2 ± 4.6	73.3 ± 22	2661	2891
13	1	298	Ne	4.6	0.52[b]	3.7	8.43	21.8 ± 6.7	90.7 ± 27	1363	1785
14	1	298	Ne	12	1.4[b]	13	20.9	15.8 ± 7.2	86.7 ± 26	2681	3698
15	1	299	Ne	3.91	0.46[b]	5.3	6.46	19.4 ± 7.9	95.0 ± 29	1035	1237
16	2.5	297	Ne	5.41	0.5[b]	4.9	6.75	9.1 ± 9	63.3 ± 19	881	1072
17	2.5	297	Ne	5.72	3.45[b]	3.5	11.6	28.8 ± 8.9	117.8 ± 35	1675	2500
18	2.5	298	Ne	6.36	3.42[a]	≈0.6	12.4	14.9 ± 15			2900
19	1	300	Ar	8.03	1.58[b]	17.3	12.6			2069	2249
20	1	300	Ar	7.03	1.5[b]	16.3	11.0			2092	2378
21	1	299	Ar	8.6	0.8[b]	3.7	16.8			2796	3455
22	1	299	Ar	3.99	0.45[b]	3.1	7.41			1390	1590
23	1	301	Ar	3.91	0.5[b]	3.8	6.1			1003	1149
24	1	300	Ar	6.02	0.66[b]	2.5	11.1			2140	2330
25	1	300	Ar	10.1	2.1[b]	21.4	17.0			2803	2957
26	1	295	Ar	5.21	0.5[b]	7.3	6.81				1209
27	1	296	Ar	0	18.1[b]	25.7	0			130	

[a] Precursor: CH_3Br. [b] Acetone.

(HCO^+) = 11.97 eV, AP(CO^+) = 14.1 eV[33]), respectively. In the Ne-lamp experiments where acetone was used as the precursor, the peak at $m/e = 14$ originating from dissociation of excited CH_3^+ into CH_2^+ was taken for the fitting procedure because the separation of the actual methyl radical signal from the acetone cracking into the same channel was not possible. For bromomethane (IE = 10.53 eV,[34] AP(CH_3^+) = 12.8 eV, AP(CH_2^+) = 14.7 eV[35]) neither channel, $m/e = 14$ nor 15, could be used so that only kinetic data from the formaldehyde formation could be obtained. The fit for formaldehyde formation was checked against the increase in the signal at $m/e = 29$, which should originate mainly from cracking of CH_2O^+ into HCO^+. For this test the formaldehyde fit for $m/e = 30$ was multiplied by the respective calibration ratio (see Table 1) resulting in the equivalent value for the $m/e = 29$ channel of the CH_2O^+ dissociation. Afterward, the offsets caused by dissociation of $CH_3COCH_3^+$ were added. The resulting profiles described the actual data very well for all experiments, confirming the fit and the identity of the $m/e = 30$ channel as formaldehyde. For the fitting procedure, the data points were shifted in time by one time step (48 μs) to account for the finite travel time of the molecules from the orifice to the ionization region.

As can be seen in Figure 6, the reaction rates obtained from the rise time of formaldehyde (shown as open triangles down) are generally larger by up to 20% compared to the rates calculated from the decrease in the CH_3 signal (solid triangles up). The most likely source of error lies in the fitting procedure (see above), for which the infinity value, $[CH_2O]_{max}$, was fixed. Even a slow loss reaction for CH_2O molecules could easily lead to an overestimate of the observed reaction rate. As a test we generated curves composed of two exponential functions mimicking a fast rise and a slow decrease and fitted single-exponential functions to these. Even small decay rates of 1−2% compared to the rate of production resulted in apparent reaction rates 5% to 10% higher. Unfortunately, we were not able to observe such small decay rates (≈10 s^{-1}) under the experimental conditions chosen. A candidate for this loss could be a temporary adsorption of formaldehyde on the reactor walls. However, second-order rate coefficients calculated separately from the methyl decay or formaldehyde increase lie within 10% of the second-order rate coefficient calculated considering all data. In general the statistical error for each evaluated rate can be given by approximately 10% (2σ) for the methyl decay and 20% (2σ) for the formaldehyde increase.

With bromomethane as precursor, the data show a large amount of scatter, which we attribute to wall reactions caused by surface contamination with bromine atoms or bromomethane itself. Therefore, only data from experiments in which acetone as precursor was used were taken for both the CH_3 decay and CH_2O increase. The overall second-order rate coefficient for the reaction $CH_3 + O(^3P) \rightarrow$ products at $P = 1$ Torr (He) and $T = (299 \pm 2)$ K is given by

$$k_1 = (1.7 \pm 0.3) \times 10^{-10}\ \text{cm}^3\ \text{molecule}^{-1}\ \text{s}^{-1}$$

in excellent agreement with the recommended value of 1.4×10^{-10} cm^3 s^{-1}.[11] The error given here is twice the standard deviation.

Product Analysis. Products of reaction 1 identified in this investigation were CH_2O and CO. The high ionization energy of CO made it necessary to use high-energy photons from a Ne discharge for ionization. Under these conditions there were several sources of the signal at $m/e = 28$: N_2^+ from background gas, CO^+ from cracking of CH_2O and acetone, and CO^+ from photolysis of acetone and finally from reaction 1c. Taking the actual counts of acetone at $m/e = 43$ and multiplying the number by the calibration ratio CR(acetone,28: acetone,43) gives the contribution to the counts in channel 28 from cracking of acetone. The amount of CO originating from acetone photolysis can be determined by multiplying the drop in acetone counts at $m/e = 43$ by CR(CO,28: acetone,43). After subtraction of all contributions, the remaining counts at $m/e = 28$ were associated with CO produced in reaction 1. Figure 5 c shows the evolution

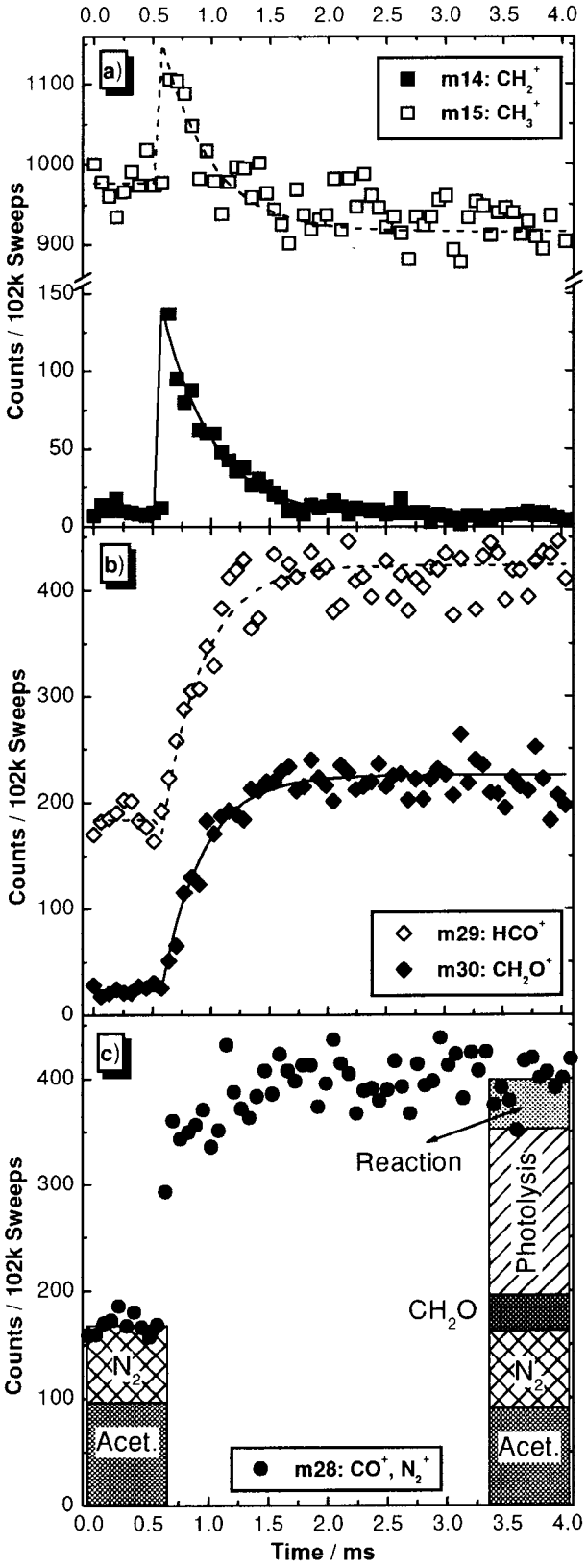

Figure 5. Ion signals of reactants and products plotted vs time recorded in experiment # 5 (see Figure 4 and Table 2). The solid lines in plots (a) and (b) are fits to second-order decay and rise functions. The broken lines were obtained by normalization of the data according to the respective calibration ratios and adjusting for different offsets. Plot (c) shows data for channel $m/e = 28$ and the contributions to the signal counts from the different sources. First-order rate constants are (a) $k' = 2521\ s^{-1}$, (b) $k'' = 3220\ s^{-1}$.

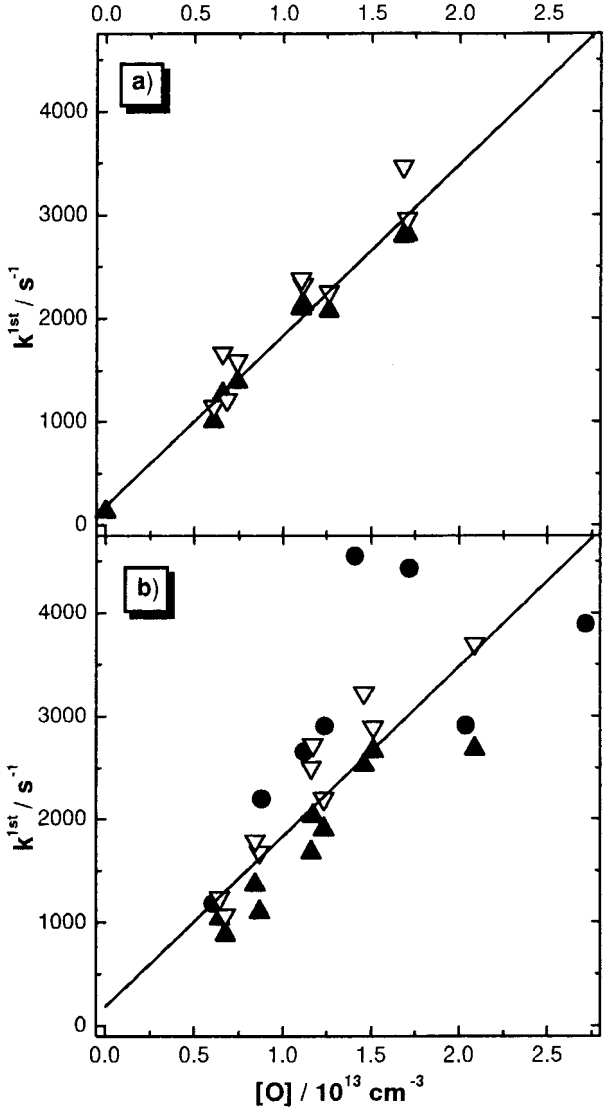

Figure 6. Second-order plot of first-order rate constants vs the concentration of oxygen atoms under various conditions. (a) Ar emission: observed were masses 15 (▲) and 30 (▽), both with acetone as precursor. (b) Ne emission: observed were mass 30 (●) with CH_3-Br as precursor, and masses 14 (▲) and 30 (▽) both with acetone as precursor. The solid line (—) in (a) and (b) is obtained by a linear fit to all first-order rate constants with acetone as a precursor.

of the signal at $m/e = 28$ and the average values before the laser fires and after reaction 1 is complete, itemized by contributions of its sources. In experiments with acetone or CH_3-Br as the precursor molecule approximately 10% or 20%, respectively, of the total counts at this mass could be attributed to CO from reaction 1.

The quantification of the yields was carried out in two different ways. First, the final amount of formaldehyde produced was compared with the drop in concentration of acetone after photolysis, assuming a methyl quantum yield of two (see Discussion on correction). Second, the increase in the CO concentration was compared to the increase in CH_2O. The concentration ratios were calculated from the differences in counts of acetone ($m/e = 43$), CH_2O ($m/e = 30$), and CO ($m/e = 28$) before the excimer laser pulse and after all methyl radicals were consumed, and corrected according to the calibration ratios from Table 1. The results are shown in Table 2 and Figure 7. The average CH_2O yield for reaction 1 was $\Phi_1(CH_2O) = 0.84 \pm 0.15$ whereas for the CO yield, a value of $\Phi_1(CO) = 0.18 \pm 0.08$ was found for $T = (299 \pm 2)$ K and $P = 1$ Torr (He), confirming the findings of Seakins and Leone.[14] These results

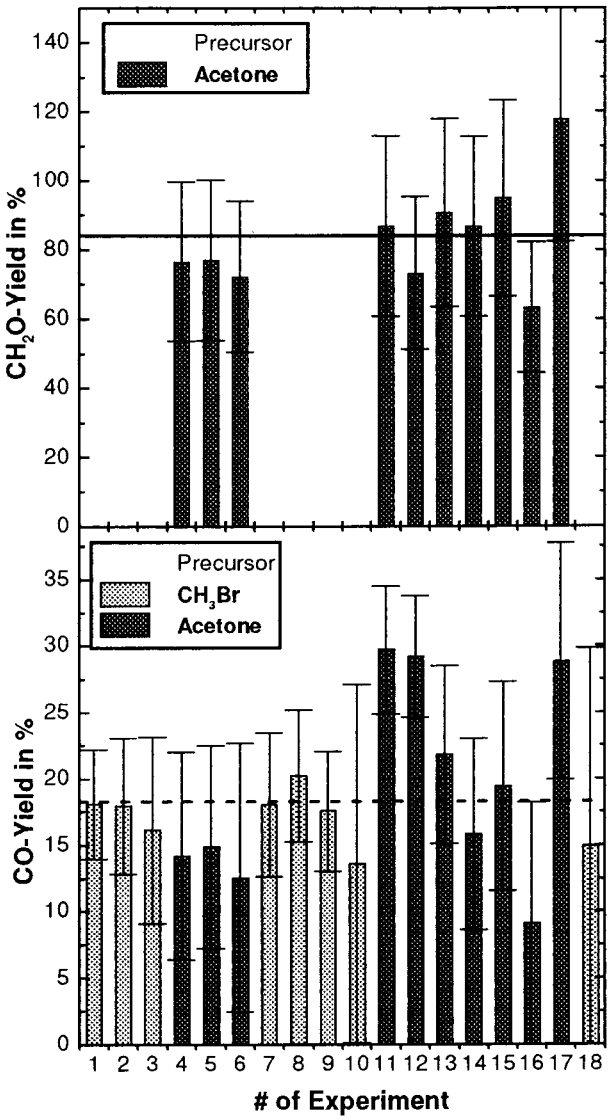

Figure 7. Plot of product yields for CH_2O and CO from reaction 1. Average values are marked by (—) and (- - -), respectively. The data are numbered according to Table 2.

also indicate that formaldehyde and carbon monoxide are the dominant carbon-containing products of reaction 1.

Discussion

Two precursor substances were used for these investigations, and each had its advantages and disadvantages. The photolysis of acetone at $\lambda = 193$ nm is essentially a clean source for methyl radicals as Lightfoot et al. showed.[36] According to these authors, the channel leading to $2CH_3 + CO$ accounts for ≈95% of the total dissociation. The apparent CO yield of reaction 1 would have to be corrected upward by approximately 14% whereas the CH_2O yield would have to be raised by 0.95^{-1} if 5% of the photolyzed acetone went into minor channels. The reported minor products are $CH_2COCH_3 + H$ (∼3%), $CH_4 + CH_2CO$ (≤ 2%), and CH_2 from secondary photolysis of methyl radicals. A subsequent reaction of CH_2COCH_3 with O atoms might lead directly or indirectly to CO or CH_2O, thus obscuring any production of carbon monoxide or formaldehyde from reaction 1. In turn, this would lower the apparent yield for both reaction products by a slight amount depending on the actual product distribution of the reaction $CH_2COCH_3 + O(^3P)$. Studies performed by North et al.[37] on acetone photolysis at $\lambda = 193$ nm did not detect either CH_4 or CH_2CO, thus confirming the upper limit given by Lightfoot et al. However, North et al. found that all detected H atoms could be attributed to secondary photolysis of methyl fragments, leaving the 3% value of the $CH_2COCH_3 + H$ channel questionable.

We attempted to detect CH_2 radicals (IE = 10.35 eV[38]) in separate experiments photolyzing acetone at the highest obtainable laser intensities. Using Ar as the discharge gas the formation of CH_2^+ from CH_3 was not possible, providing a low background for the detection of CH_2 radicals. At bath gas (He) pressures of 1 Torr, electronically excited singlet CH_2 should be quickly quenched ($\tau \approx 10\ \mu s$[39]) into the less reactive ground triplet state. Assuming a reactive removal of singlet methylene on every collision with acetone, less than 50% of the CH_2 produced is supposed to elude detection. However, even at methyl radical concentration of larger than 1×10^{13} molecules cm^{-3} no signal at $m/e = 14$ could be observed. Assuming that the ionization cross section of CH_2 is comparable to that of CH_3, we concluded that the photon density was not high enough to produce methylene radicals in any significant amount.

As mentioned earlier, the chemistry of the system with bromomethane as the precursor species does not appear to be as clean as in the case with acetone. We assume that heterogeneous reactions on the reactor walls involving bromine species are responsible for the observed fluctuations in the reaction rate, so that it is unlikely that the products are either CO or CH_2O. Therefore, the measured concentration ratio of these species should simply reflect exactly the product distribution of reaction 1. As can be seen in Figure 7, consistent yields of CO were determined from experiments using either CH_3Br or acetone as a methyl radical precursor.

Since ethane produces a strong dissociative ionization signal at $m/e = 28$, we also considered the effect of methyl radical recombination to ethane as a possible contribution to the total signal at $m/e = 28$. Calculations based on rate coefficients and measured ionization efficiencies suggest the effect should be undetectable at our noise levels. Furthermore, no correlation exists between the $[O]/[CH_3]$ ratio and the computed CO yield, justifying the neglect of corrections for ethane formation and dissociative ionization.

The surface adsorption of formaldehyde mentioned above would definitely alter the measured CH_2O and CO yields directly. However, it is very unlikely that the loss amounted to more than a few percent, and even with an unrealistic correction for the formaldehyde yield to 100%, the yield for CO (which depends on the [CO] to $[CH_2O]$ ratio), would drop only to 85% of its calculated value.

Averaging all measured product yields of CO from reaction 1, $\Phi_1(CO)$, including the results for the formaldehyde yield with $\Phi_1(CO) = 1 - \Phi_1(CH_2O)$ results in

$$\Phi_1(CO) = 0.17 \pm 0.11$$

for $T = (299 \pm 2)$ K and $P = 1$ Torr (He). The error given is one standard deviation. Correcting the product yield according to the quantum yield measured by Lightfoot et al. would lower $\Phi_1(CO)$ by less than 10%, which lies well inside the error limits.

Another source of error might come from reactions of vibrationally excited photolysis products. A number of authors have investigated the energy distribution in the photofragments produced in the photolysis of acetone at $\lambda = 193$ nm.[37,40,41] The internal energy in the methyl fragments is considerable (E_{int} = 98.7 kJ/mol)[37] which might influence the dynamics as well as kinetics of reactions 1. However, deactivation through collisions with the bath gas, He,[42,43] or the reactor walls is

sufficiently fast, resulting in a lifetime of vibrationally excited methyl radical of $\tau \leq 100\ \mu$s. The time constant for the reaction is up to 10 times longer than that for deactivation, so that a possible influence on the mechanism for reaction 1 should be minimal. Moreover, a few experiments were performed at bath gas pressures of $P = 2.5$ Torr, accelerating the deactivation without any detectable effect on kinetics or product distribution.

The literature on the photodissociation dynamics of bromomethane at $\lambda = 193$ nm is unfortunately very sparse. Van Veen et al.[44] investigated the translational energy distribution in the methyl and bromine fragments and concluded that the internal energy in the CH_3 fragments is considerably less than in the case of acetone photodissociation ($E_{int} = 30.6$ and 18.5 kJ/mol for the Br/Br* channels). Most of the excitation is in the ν_2 (CH_2 umbrella) vibrations, which are quenched much faster by He atoms than the ν_3 (antisymmetric C−H stretch) vibration.[42,43] In terms of dynamical properties, CH_3Br is definitely favored over acetone, but the presence of bromine compounds tends to introduce some disadvantages (see above).

The photoionization of the CO product at Ne wavelengths also needs additional treatment. The absorption spectrum of ground-state $CO(X^1\Sigma^+)$ is very structured in this region, stemming from Rydberg transitions converging to the $CO^+(A^2\Pi)$ state together with non-Rydberg transitions and an underlying photoionization continuum.[45,46] According to Cook et al.[45] the bands are subject to preionization with an efficiency around 20%. Keeping in mind that the CO produced in reaction 1 can be highly vibrationally excited[14] the measured $CO(v)$ ensemble might exhibit a different overall ionization efficiency after absorption of a VUV photon than a thermalized ensemble. Although Rydberg states might be accessible from vibrationally excited CO it seems unlikely to find this situation realized. It is also conceivable that the vibrational excitation leads to an enhanced dissociation of CO into neutral fragments instead of ionization resulting in an underestimation of the measured product yield. All these effects of the vibrational population of CO are difficult to predict exactly but were considered to be small and generally omitted in the error analysis. This problem will be addressed in the future by using the He line at 21.22 eV for ionization because the absorption spectrum for CO above 60 nm becomes flat and the ion yield approaches unity. Any vibrational excitation should therefore not alter the ionization efficiency.

Concerning a possible mechanism for reactions 1, we refer to the paper of Seakins and Leone.[14] The initial step is supposed to be the association of CH_3 and $O(^3P)$ to form an activated methoxy radical, CH_3O^*, with internal energy of approximately 380 kJ/mol above the ground state. This is enough energy to overcome barriers to elimination of either H atoms, leading to CH_2O, or molecular hydrogen, leaving an energized HCO* radical behind which might subsequently eliminate another H atom, leading to CO. Other possible pathways include isomerization of CH_3O^* to CH_2OH^* followed by stepwise elimination of H_2 and H atoms. However, as Seakins and Leone pointed out, there is either considerable disagreement about the barrier heights of the various transition states, or information about them is not available at all.

Summary

The reaction of methyl radicals with oxygen atoms has been investigated with a new apparatus. TOF mass spectrometry combined with a special grid assembly at the entrance of the flight tube that allows extraction of ions at a high repetition rate and an efficient counting apparatus make the simultaneous observation of the kinetics and mechanism of fast radical−radical reactions possible. The reaction of methyl radicals and oxygen atoms was investigated. The results of Seakins and Leone,[14] showing the existence of a second reaction channel producing carbon monoxide, was confirmed. The 17% yield determined in this work would indicate that a nonnegligible amount of the CO formed in important combustion systems would come directly from reactions 1. The remaining ≈80% would have to be produced in an oxidation chain beginning with CH_2O. The exact influence on flame properties can only been determined in simulation calculations. Further experiments, especially on the temperature dependence of the branching ratio, are necessary to establish these results under more combustion-relevant conditions and are planned for the future.

Acknowledgment. The authors thank Dr. Herbert J. Bernstein for fruitful discussions and assistance in designing and assembling the data acquisition system. This work was carried out at Brookhaven National Laboratory under Contract DE-AC02-98CH10886 with the U.S. Department of Energy and supported by its Division of Chemical Sciences, Office of Basic Energy Sciences.

References and Notes

(1) Miller, J. A.; Kee, R. J.; Westbrook, C. K. *Annu. Rev. Phys. Chem.* **1990**, *41*, 345.
(2) Warnatz, J.; Mass, U.; Dibble, R. W. *Combustion: Physical and Chemical Fundamentals, Modeling and Simulation, Experiments, Pollutant Formation*; Springer: Berlin Heidelberg New York, 1996.
(3) Niki, H.; Daby, F. E.; Weinstock, B. *J. Chem. Phys.* **1968**, *48*, 5729.
(4) Washida, N. *J. Chem. Phys.* **1980**, *73*, 1665.
(5) Plumb, I. C.; Ryan, K. R. *Int. J. Chem. Kinet.* **1982**, *14*, 861.
(6) Slagle, I. R.; Sarzynski, D.; Gutman, D. *J. Phys. Chem.* **1987**, *91*, 4375.
(7) Oser, H.; Walter, D.; Stothard, N. D.; Grotheer, O.; Grotheer, H. H. *Chem. Phys. Lett.* **1991**, *181*, 521.
(8) Atkinson, R.; Baulch, D. L.; Cox, R. A.; R. F. Hampson, J.; Kerr, J. A.; Troe, J. *J. Phys Chem. Ref. Data* **1992**, *21*, 1125.
(9) Tsang, W. *Heats of Formation of Organic Free Radicals by Kinetic Methods in Energetics of Organic Free Radicals*; Simoes, J. A. M., Greenberg, A., Liebman, J. F., Eds.; Blackie Academic and Professional: London, 1996; p 22.
(10) Chase, M. W., Jr.; Davies, C. A.; Downey, J. R., Jr.; Frurip, D. J.; McDonald, R. A.; Syverud, A. N. *J. Phys. Chem. Ref. Data, Suppl. 1* **1985**, *14*, 1.
(11) Baulch, D. L.; Cobos, C. J.; Cox, R. A.; Frank, P.; Hayman, G.; Just, T.; Kerr, J. A.; Murrels, T.; Pilling, M. J.; Troe, J.; Walker, R. W.; Warnatz, J. *J. Phys. Chem. Ref. Data* **1994**, *23*, 847.
(12) Koda, S.; Endo, Y.; Tsuchiya, S.; Hirota, E. *J. Chem. Phys.* **1991**, *95*, 1241.
(13) Erman, P.; Karawajczyk, A.; Rachlew-Kallne, E.; Stromholm, C.; Larsson, J.; Persson, A.; Zerne, R. *Chem. Phys. Lett.* **1993**, *215*, 173.
(14) Seakins, P. W.; Leone, S. R. *J. Phys. Chem.* **1992**, *96*, 4478.
(15) Slagle, I. R.; Yamada, F.; Gutman, D. *J. Am. Chem. Soc.* **1981**, *103*, 149.
(16) Slagle, I. R.; Gutman, D. *J. Am. Chem. Soc.* **1985**, *107*, 5342.
(17) Slagle, I. R.; Sarzynski, D.; Gutman, D.; Miller, J. A.; Melius, C. F. *J. Chem. Soc., Faraday Trans. 2* **1988**, *84*, 491.
(18) Fockenberg, C.; Bernstein, H. J.; Hall, G. E.; Muckerman, J. T.; Preses, J. M.; Sears, T. J.; Weston, R. E. J. *Rev. Sci. Instr.* **1999**, in press.
(19) Manatt, S. L.; Lane, A. L. *J. Quant. Spectrosc. Radiat. Trans.* **1993**, *50*, 267.
(20) Phillips, L. F. *J. Phys. Chem.* **1981**, *85*, 3994.
(21) Snow, K. B.; Thomas, T. F. *Int. J. Mass Spectrom. Ion Processes* **1990**, *96*, 49.
(22) Norwood, K.; Ng, C. Y. *Chem. Phys. Lett.* **1989**, *156*, 145.
(23) Kelly, R. L. *J. Phys. Chem. Ref. Data* **1987**, *16*, 337.
(24) Trott, W. M.; Blais, N. C.; Walters, E. A. *J. Chem. Phys.* **1978**, *69*, 3150.
(25) Powis, I.; Danby, C. J. *Int. J. Mass Spectrom. Ion Phys.* **1979**, *32*, 27.
(26) Berkowitz, J.; Ellison, G. B.; Gutman, D. *J. Phys. Chem.* **1994**, *98*, 2744.
(27) Ohno, K.; Okamura, K.; Yamakado, H.; Hoshino, S.; Takami, T.; Yamauchi, M. *J. Phys. Chem.* **1995**, *99*, 14247.
(28) Herron, J. T.; Huie, R. E. *Chem. Phys. Lett.* **1980**, *76*, 322.

(29) Singleton, D. L.; Cvetanovic, R. J. *J. Phys. Chem. Ref. Data* **1988**, *17*, 1377.
(30) James, F. C.; Kerr, J. A.; Simons, J. P. *J. Chem. Soc., Faraday Trans. 1* **1973**, *69*, 2124.
(31) Callear, A. B.; Cooper, I. A. *J. Chem. Soc., Faraday Trans.* **1990**, *86*, 1763.
(32) Chupka, W. A.; Lifshitz, C. *J. Chem. Phys.* **1968**, *48*, 1109.
(33) Guyon, P. M.; Chupka, W. A.; Berkowitz, J. *J. Chem. Phys.* **1976**, *64*, 1419.
(34) Kimura, K.; Katsumata, S.; Achiba, Y.; Yamazaki, T.; Iwata, S. Ionization energies, Ab initio assignments, and valence electronic structure for 200 molecules. In *Handbook of HeI Photoelectron Spectra of Fundamental Organic Compounds*; Japan Scientific Soc. Press: Tokyo, 1981.
(35) Kaposi, O.; Riedel, M.; Vass-Balthazar, K.; Sanchez, G. R.; Lelik, L. *Acta Chim. Acad. Sci. Hung.* **1976**, *89*, 221.
(36) Lightfoot, P. D.; Kirwan, S. P.; Pilling, M. J. *J. Phys. Chem.* **1988**, *92* (2), 4938.
(37) North, S. W.; Blank, D. A.; Gezelter, J. D.; Longfellow, C. A.; Lee, Y. T. *J. Chem. Phys.* **1995**, *102*, 4447.
(38) Reineke, W.; Strein, K. *Ber. Bunsen-Ges. Phys. Chem.* **1976**, *80*, 343.
(39) Ashfold, M. N. R.; Fullstone, M. A.; Hancock, G.; Ketley, G. W. *Chem. Phys.* **1981**, *55*, 245.
(40) Donaldson, D. J.; Leone, S. R. *J. Chem. Phys.* **1986**, *85*, 817.
(41) Hall, G. E.; Vanden Bouten, D.; Sears, T. J. *J. Chem. Phys.* **1991**, *94*, 4182.
(42) Callear, A. B.; Van den Bergh, H. E. *Chem. Phys. Lett.* **1970**, *5*, 23.
(43) Donaldson, D. J.; Leone, S. R. *J. Phys. Chem.* **1987**, *91*, 3128.
(44) Van Veen, G. N. A.; Baller, T.; De Vries, A. E. *Chem. Phys.* **1985**, *92*, 59.
(45) Cook, G. R.; Metzger, P. H.; Ogawa, M. *Can. J. Phys.* **1965**, *43*, 1706.
(46) Ogawa, M.; Ogawa, S. *J. Mol. Spectrosc.* **1972**, *41*, 393.